

## Original Article

# Preparation of magnetic nanoparticles co-carrying tissue inhibitor of metalloproteinase-2 and cisplatin and the inhibitory effects on liver cancer HepG2 cells

Liping Hu<sup>1\*</sup>, Yigubali-Aibaidula<sup>1\*</sup>, Dongmei Qin<sup>2</sup>, Nulibiya-Abudukeyoumu<sup>1</sup>, Guolun Du<sup>1</sup>, Yuexin Zhang<sup>1</sup>, Maimaitiaili-Wubuli<sup>1</sup>

<sup>1</sup>Department of Infectious Diseases, First Affiliated Hospital of Xinjiang Medical University, Urumqi 830054, P. R. China; <sup>2</sup>School of Pharmacy, Shihezi University, Shihezi 832002, P. R. China. \*Equal contributors.

Received January 16, 2016; Accepted April 6, 2016; Epub June 15, 2016; Published June 30, 2016

**Abstract:** Background: To prepare magnetic nanoparticles (MNP) co-carrying tissue inhibitor of metalloproteinase-2 (TIMP-2) and cisplatin (CDDP), and to evaluate the inhibitory effects of the nanoparticles (MNP-CDDP/TIMP-2) on liver cancer HepG2 cells. Methods: MNP-CDDP/TIMP-2 was prepared through electrostatic adsorption of CDDP-loaded magnetic nanoparticles (MNP-CDDP) and TIMP-2-bound poly (ethylene glycol) monomethyl ether-polyethyleneimine (MPEG-PEI). The structure, particle size and zeta potential were characterized by infrared spectroscopy, transmission electron microscopy and laser particle size analyzer. CDDP content was detected by the o-phenylenediamine method. Gene transfection efficiency and transfection of TIMP-2 were detected by flow cytometry. TIMP-2 mRNA and protein expressions in HepG2 cells after transfection were detected with RT-PCR and Western blot respectively. The effects of MNP-CDDP/TIMP-2 on the proliferation, apoptosis and invasion of HepG2 cells were assessed with CCK-8 assay, flow cytometry and Matrigel invasion assay. Results: The hydrodynamic particle size was 151.3 nm, and the zeta potential was +14.7 mV. The average CDDP content of MNP-CDDP/TIMP-2 was 120 µg/mL, and the encapsulation efficiency was 33.2%. After transfection with TIMP-2 plasmid in HepG2 cells, the TIMP-2 mRNA and protein expression levels significantly increased. The MNP-CDDP/TIMP-2 group had significantly higher growth inhibition rate (34.9%) and apoptotic rate (43.4%) than those of MNP-CDDP (27.1% and 38.0%) and (MPEG-PEI) TIMP-2 (18.9% and 16.2%) groups (P<0.05). In the MNP-CDDP/TIMP-2 group, 27±3 cells penetrated the Matrigel membrane, which was significantly less than that of the control group (P<0.05), suggesting that the invasion and migration capacities decreased. Conclusion: Magnetic nanoparticles co-carrying TIMP-2 and CDDP were successfully prepared, which exerted obvious inhibitory effects on liver cancer cells *in vitro*.

**Keywords:** Magnetic nanoparticle, tissue inhibitor of metalloproteinase-2, cisplatin, liver cancer

## Introduction

As one of the most common malignant tumors worldwide, liver cancer has the incidence rate and mortality rate ranking 5th and 3rd respectively [1]. By specifically binding activated matrix metalloproteinases (MMPs) and inhibiting their activities, tissue inhibitor of metalloproteinase-2 (TIMP-2) can suppress the growth and distant metastasis of tumors. TIMP-2 expressions decrease in lung cancer [2] and colon cancer [3] tissues, which promote the invasion and metastasis of tumors because it evidently inhibits their growth and angiogenesis [3].

Cisplatin (CDDP), as one of the first-choice chemotherapeutic drugs for advanced cancers, has limited antitumor effects due to low water solubility, high toxicity to normal tissues and drug resistance. With high biocompatibility, stability and superparamagnetism, magnetic nanoparticles (MNP) have been used to load CDDP (MNP-CDDP), which inhibits the invasion of tumor cells *in vitro* [4]. In this study, MNP-CDDP and TIMP-2 bound poly (ethylene glycol) monomethyl ether-polyethyleneimine (MPEG-PEI) were employed to prepare MNP-CDDP/TIMP-2 that simultaneously allowed chemotherapy and gene therapy of liver cancer.

## Materials and methods

### Reagents

PEI (dendritic, molecular weight: 25 kDa), dicyclohexylcarbodiimide (DCC), N-hydroxysuccinimide (NHS, analytically pure), MPEG (molecular weight: 2 kDa), dimethylformamide (DMF),  $\text{FeCl}_3 \cdot 6\text{H}_2\text{O}$  (analytically pure),  $\text{FeSO}_4 \cdot 4\text{H}_2\text{O}$  (analytically pure) and food-grade sodium alginate were purchased from Sigma (St. Louis, USA). CDDP was bought from Qilu Pharmaceutical Co., Ltd. (Shandong Province, China). HepG2 cells were obtained from China Center for Type Culture Collection (Wuhan, China). RPMI1640 culture medium, fetal bovine serum and trypsin were provided by Gibco (MD, USA). TIMP-2 plasmid was purchased from Shanghai GenePharma Co., Ltd. (China). Plasmid maxi preparation kit and BCA protein kit were bought from Life Technologies (MD, USA). Celling Counting Kit-8 (CCK-8) kit was obtained from Dojindo Laboratories (Tokyo, Japan). Transwell culture plates were provided by Corning (NY, USA). TIMP-2 antibody was purchased from Santa Cruz (CA, USA). SYBR® Premix Ex TaqTMII was bought from Tli RNaseH Plus. RNAiso plus was obtained from TaKaRa (Tokyo, Japan).

### Apparatus

Brookhaven Zeta Plus laser particle size analyzer was provided by Brookhaven (CA, USA). UVIKON923 UV-vis spectrophotometer and PCR system were purchased from Eppendorf (NY, USA). Electrophoresis system was bought from Beijing Liuyi Instrument Factory.

### Preparation of MNP-CDDP/TIMP-2

MPEG (10 g) and succinic anhydride (2.5 g) were vacuum-dried for 24 h, dissolved in dried DMF, reacted in a nitrogen atmosphere at 75°C and refluxed for 8 h. The product was dialyzed (molecular weight cut-off: 500) for 3 d, with water refreshed every 12 h, then freeze-dried, and identified as MPEG-COOH by using infrared (IR) spectroscopy. Afterwards, MPEG-PEI copolymer was prepared through dehydration condensation between MPEG-COOH and PEI rich in amino groups. Briefly, 5.0 g PEI and 2.0 g MPEG-COOH were dissolved in dimethyl sulfoxide, into which 0.6 g DCC and 0.35 g NHS were added to be reacted at room temperature for 24 h. The product was dialyzed in deionized

water for 3 d (molecular weight cut-off: 8000) and freeze-dried as MPEG-PEI. Then the copolymer was dissolved in water, mixed with plasmid (TIMP-2) in the mass ratio of 5:1 and vortexed for 20 min, giving (MPEG-PEI) TIMP-2. (MPEG-PEI) TIMP-2 was thereafter mixed with MNP-CDDP prepared as previously reported [4] in the mass ratio of 4:1 and vortexed for 30 min, yielding MNP-CDDP/TIMP-2.

### Characterizations of MNP-CDDP/TIMP-2

*Observation of morphology by transmission electron microscopy (TEM):* MNP-CDDP/TIMP-2 was suspended in deionized water, diluted 5-fold, ultrasonically shaken at 200 W for 3 min, dropped onto a coated copper mesh, dried at room temperature and observed by TEM.

*Characterization of MPEG-COOH by FT-IR spectroscopy:* MPEG-COOH was freeze-dried and characterized by FT-IR spectroscopy from 500 to 4000  $\text{cm}^{-1}$  with the resolution of 4  $\text{cm}^{-1}$ .

*Detection of particle size and zeta potential:* MNP-CDDP/TIMP-2 was diluted with deionized water and ultrasonically shaken. Effective particle size and zeta potential were detected by laser particle size analyzer.

*Detection of CDDP content in MNP-CDDP/TIMP-2 by the o-phenylenediamine (OPDA) method:* Sample (6 mL) was added in 6 mL of OPDA/DMF solution, boiled in water bath for 10 min and rapidly cooled, with the absorbance measured at 703 nm to detect the CDDP content after being compared with the standard curve. Encapsulation efficiency (EE) was calculated according to the following formula:  $\text{EE} (\%) = \text{CDDP content} / \text{total CDDP content} \times 100\%$ .

### Detection of binding of MNP to plasmid by agarose gel electrophoresis

MNP were divided into two groups. Group I: MNP and plasmids were subjected to electrostatic adsorption in different ratios, mixed by vortexing and resolved by agarose gel electrophoresis. Group II: Empty plasmid, empty plasmid + DNase-I + MNP, and plasmid + DNase-I were incubated at room temperature for 30 min respectively. Bromophenol blue-containing loading buffer (1  $\mu\text{L}$ ) was added to 6  $\mu\text{L}$  of the mixture each, resolved by 1% agarose gel electrophoresis at 60 V for 30 min, and observed

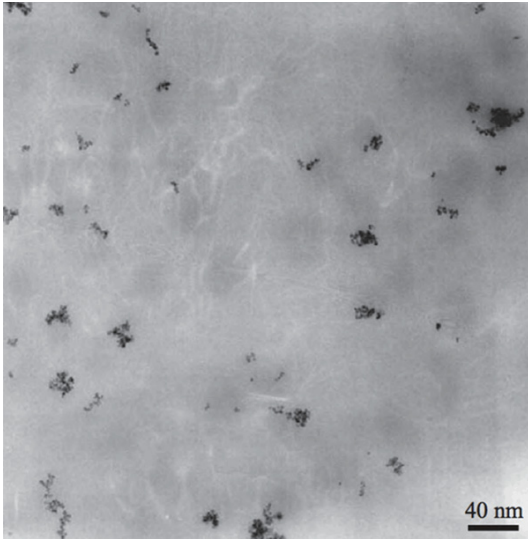


**Figure 1.** TEM image of MNP-CDDP/TIMP-2.

under a UV lamp. The experiments were performed in triplicate.

#### *Detection of TIMP-2 expressions in cells by RT-PCR and Western blot*

HepG2 cells were cultured in 6-well plates and divided into an experimental (MNP-CDDP/TIMP-2) group, a negative control (MNP/TIMP-2) group and a positive control (PEI/TIMP-2) group.

The supernatant was discarded 48 h after transfection, and total RNA was extracted after addition of Trizol. Primers: GAPDH: F: 5'-AAGGTGGTGAAGCAGGCGGC-3'; R: 5'-GAGCAATGCAGCCCCAGCA-3'. TIMP-2: F: 5'-TGACGCTCCCGGTGCAC-3'; R: 5'-TGCTGAAGAGGGGGCCGTGTAGAT-3'.

PCR reactants were added in the PCR reaction system and pre-denatured at 95°C for 30 s by using SYBR® Premix Ex Taq™ (Tli RNaseH Plus) kit. PCR reaction was conducted at 95°C for 5 s and at 60°C for 30 s (40 cycles in total). After extension and the reaction, amplification and melting curves were plotted, and PCR quantification was performed to plot the standard curve.

HepG2 cells were washed with PBS and collected 48 h after transfection, TIMP-2 protein expressions in which were detected by Western blot. Mouse anti-human TIMP-2 antibody (1:1500 diluted) and HRP-labeled goat anti-mouse IgG antibody (1:5000 diluted) were used

as primary and secondary antibodies respectively. Chemiluminescence detection was employed with a luminescence imaging system. By using the image analysis system, light intensities of the proteins were compared with that of the control protein. GAPDH was used as the internal reference.

#### *Detection of in vitro cytotoxic effects of MNP-CDDP/TIMP-2 and apoptosis of liver cancer cells*

*Detection of cell proliferation capacities before and after drug treatment by CCK-8 assay:* HepG2 cells in the logarithmic growth phase were inoculated onto 96-well plates at the density of  $1 \times 10^5$ /mL (100  $\mu$ L/well), cultured for 24 h, and divided into a control group, a zeroing well (only contained culture medium), and experimental groups ((MPEG-PEI) TIMP-2, MNP-CDDP, MNP-CDDP/TIMP-2). CCK-8 (10  $\mu$ L) was added into each well to further culture the cells for 2 h. The absorbance at 450 nm (D450) was measured by a microplate reader. Then the proliferation inhibition rate was calculated according to the following formula: Proliferation inhibition rate (%) =  $1 - [D(\text{Drug treatment}) - D(\text{Blank})] / [D(\text{Control}) - D(\text{Blank})] \times 100\%$ .

*Detection of cell apoptosis by flow cytometry:* HepG2 cells in the logarithmic growth phase were inoculated onto 6-well plates at the density of  $1 \times 10^5$ /mL (2 mL/well) and cultured for 24 h. Afterwards, the supernatant was discarded, and the cells were co-cultured with MNP-CDDP/TIMP-2 diluted by complete culture medium, collected and divided in half. Flow cytometry was carried out for one half to detect the transfection efficiency of plasmids, with the TIMP-2 group as control. According to the instructions of Annexin V FITC-A kit, flow cytometry was performed for the other half, with MNP, MNP-CDDP and (MPEG-PEI) TIMP-2 groups as controls.

#### *Detection of cell invasion capacities before and after transfection by Matrigel assay*

Matrigel gel was evenly spread onto a polycarbonate film in Transwell chambers, which then quickly polymerized. HepG2 cells in the logarithmic growth phase were inoculated onto 24-well plates at the density of  $1 \times 10^5$ /mL (500  $\mu$ L/well) and grown adhering the wall for 24 h. After the supernatant was discarded, the cells were co-cultured with 30  $\mu$ L of MNP-

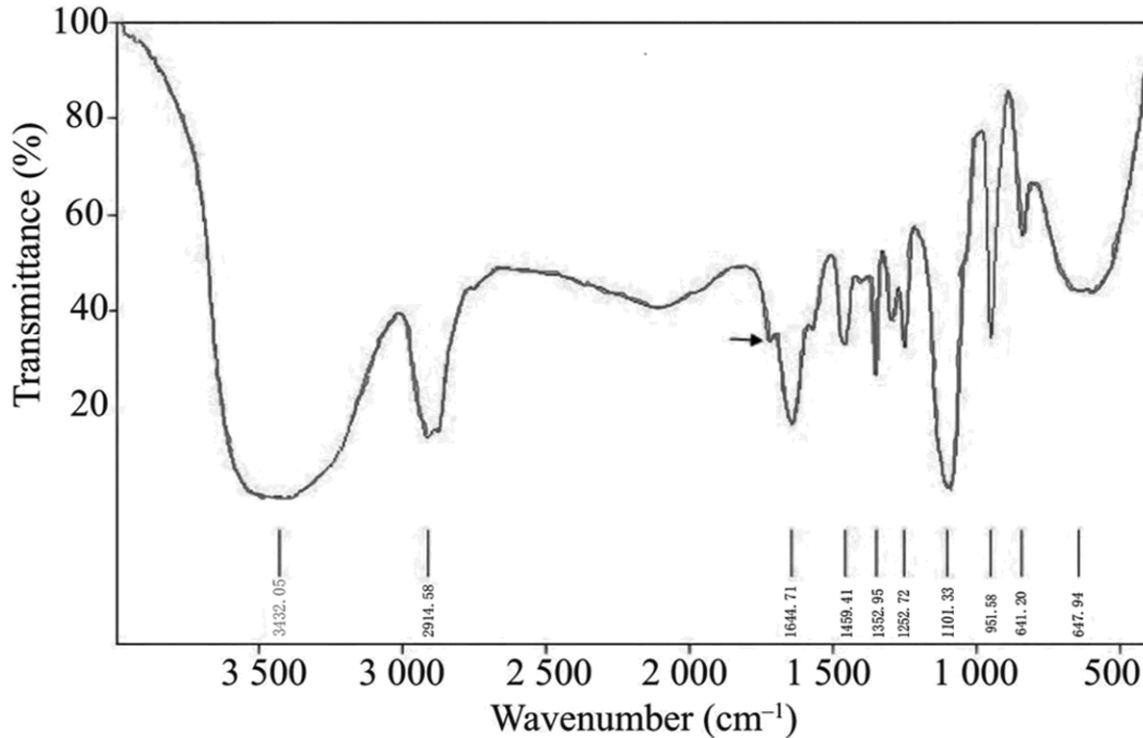


Figure 2. IR spectrum of MPEG-COOH.

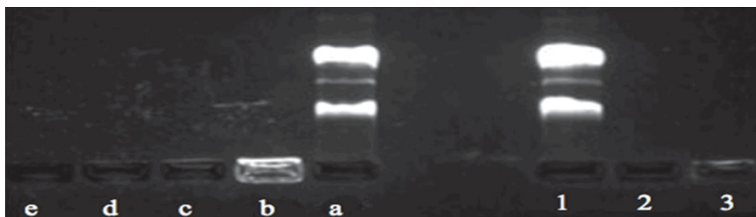


Figure 3. Agarose gel electrophoresis of binding between MNP and plasmid. The ratios of MNP to plasmid in a, b, c, d and e were 0:10, 10:10, 10:2, 10:1 and 10:0 respectively. 1: Empty plasmid; 2: plasmid + DNase-I; 3: plasmid + DNase-I + MNP.

CDDP/TIMP-2 diluted by complete culture medium for 12 h. Subsequently, the supernatant was discarded, and the cells were digested, diluted with RPMI1640 culture medium, and added in upper chambers at the density of  $1 \times 10^5/\text{mL}$  (100  $\mu\text{L}/\text{chamber}$ ). Meanwhile, 500  $\mu\text{L}$  of RPMI1640 culture medium containing 5.0% serum was added into the lower chamber. MNP, MNP-CDDP and (MPEG-PEI) TIMP-2 groups were employed as controls. The chambers were taken out 24 h later, and non-penetrating cells in the upper chambers and Matrigel gel were wiped off with sterile cotton swabs. Then the chambers were fixed in 4% paraformaldehyde, rinsed with PBS and stained with crystal violet. Afterwards, the cells on the back

of the membrane were counted. Five visual fields were randomly selected to obtain the mean. Invasion inhibition rate (%) = (1-invaded cells in the experimental group/invaded cells in the control group)  $\times$  100%.

#### Statistical analysis

All data were analyzed by SPSS13.0 and expressed as mean  $\pm$  standard deviation. Means of two groups were compared by using independent samples t-test, and pairwise comparisons among means were performed with one-way analysis of variance.  $P < 0.05$  was considered statistically significant.

## Results

### Characterizations of MNP-CDDP/TIMP-2

Left still at room temperature, MNP-CDDP/TIMP-2 were pale brown and highly mobile, without showing obvious precipitates within 3 months. TEM showed that the nanoparticles were uniformly dispersed, each of which was

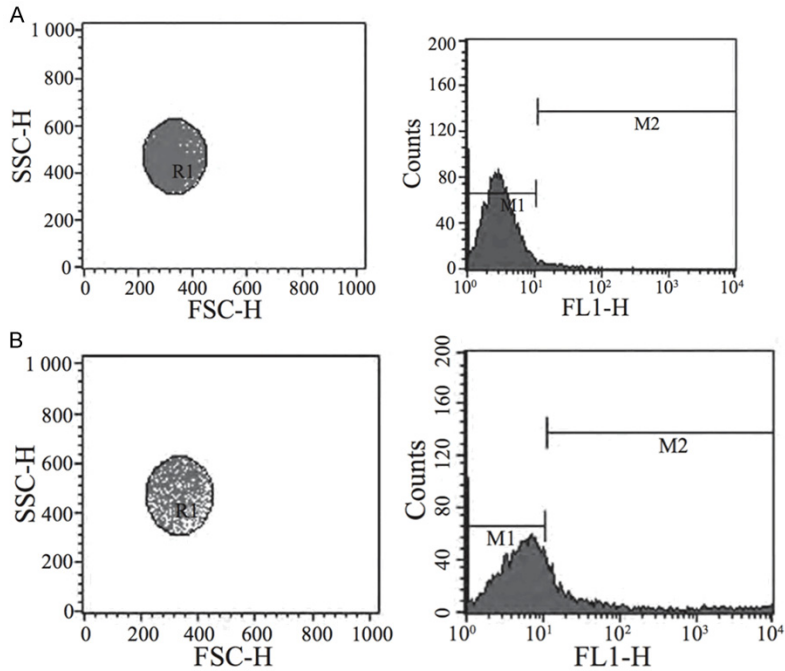


**Figure 4.** Transfection efficiencies detected by flow cytometry. A: TIMP-2 control group; B: MNP-CDDP/TIMP-2 experimental group.

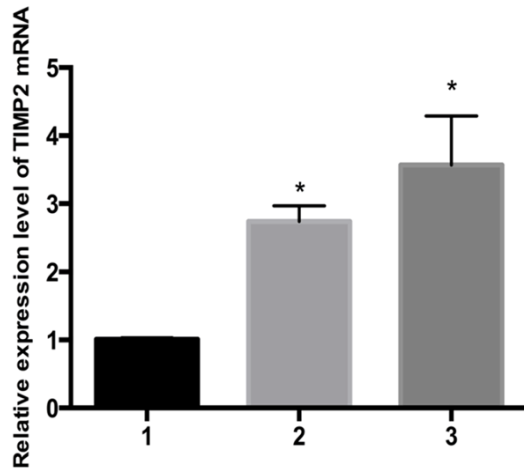


**Figure 5.** TIMP-2 mRNA expressions detected by RT-PCR. 1: MNP/TIMP-2 group; 2: MNP-CDDP/TIMP-2 group; 3: PEI/TIMP-2 group. Compared with the MNP/TIMP-2 group, \*P<0.05.

sized approximately 13 nm (Figure 1). As evidenced by the stretching vibration of -COOH at 1700 cm<sup>-1</sup> in IR spectrum (Figure 2, indicated by arrow), COOH was successfully bound to MPEG. MNP-CDDP/TIMP-2 had the particle size of 151.3 nm and the zeta potential of +14.7 mV. CDDP content was measured by using the OPDA method. The standard curve was plotted,

and the regression equation was calculated as  $Y$  (Absorbance) = 0.0045 × (Concentration) + 0.0043, RZ = 0.9893. The loading and EE of CDDP were calculated as 120 µg/mL and 33.2% respectively.

Agarose gel electrophoresis (Figure 3) showed that empty plasmid was clearly discernible in lane 1. Since empty plasmid disappeared in lane 2, it had been digested by DNase-I. Without any band, lane 3 had plasmid in the loading well, suggesting that the plasmid was adsorbed and encapsulated by MNP to protect DNase-I from damage. The ratios of MNP to plasmid in a, b, c, d and e were 0:10, 10:10, 10:2, 10:1 and 10:0 respectively.

Therefore, plasmid was well encapsulated by MNP when the mass ratio of MNP/plasmid ≥5:1.

#### Transfection of MNP-CDDP/TIMP-2

Flow cytometry showed that the transfection efficiency of plasmid in the experimental group (22.9%) was significantly higher than that of the control group (7.7%) (Figure 4). RT-PCR showed that the relative expression level of TIMP-2 mRNA in the MNP-CDDP/TIMP-2 group was significantly higher than that of the MNP/TIMP-2 group (1.7-fold) but was significantly lower than that of the PEI/TIMP-2 group (Figure 5). Western blot exhibited similar results of TIMP-2 protein expression (Figure 6).

#### In vitro inhibitory effects of MNP-CDDP/TIMP-2 on HepG2 cells

In the presence of CDDP at the final concentration of 5 µg/mL, the 24 h inhibition rate of the MNP-CDDP/TIMP-2 group was 34.9%, exceeding those of MNP-CDDP (27.1%) and (MPEG-PEI) TIMP-2 groups (19.0%). Thus, HepG2 cells were inhibited by MNP-CDDP/TIMP-2 most significantly (P<0.05) in a dose-dependent manner (Figure 7).

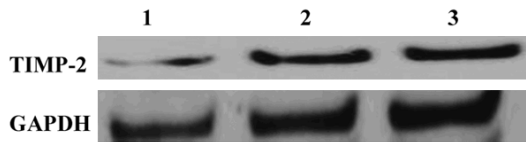


**Figure 6.** TIMP-2 protein expressions detected by Western blot. 1: MNP/TIMP-2 group; 2: MNP-CDDP/TIMP-2 group; 3: PEI/TIMP-2 group.

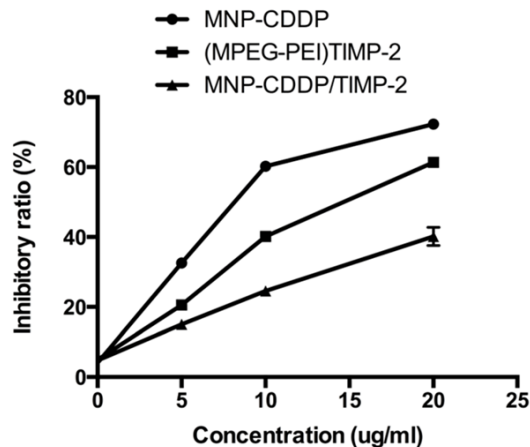


**Figure 7.** Inhibitory effects of MNP-CDDP/TIMP-2 on the growth of HepG2 cells.

When the final concentration of CDDP was 5  $\mu\text{g}/\text{mL}$ , the 24 h apoptotic rate of the MNP-CDDP/TIMP-2 group was  $43.4\% \pm 3.23\%$ , surpassing those of MNP-CDDP ( $38.0\% \pm 2.15\%$ ) and (MPEG-PEI) TIMP-2 groups ( $16.2\% \pm 3.61\%$ ) ( $P < 0.05$ ) (**Figure 8**).

Matrigel invasion assay exhibited that  $56 \pm 3$  (**Figure 9A**),  $43 \pm 3$  (**Figure 9B**) and  $47 \pm 4$  (**Figure 9C**) cells in MNP, MNP-CDDP and (MPEG-PEI) TIMP-2 groups penetrated the membrane respectively, which significantly exceeded those in the MNP-CDDP/TIMP-2 group ( $27 \pm 3$ ) (**Figure 9D**) ( $P < 0.05$ ).

## Discussion

MNP have been applied in the medical field to treat and to diagnose cancers owing to the advantages of nanoparticles as well as superparamagnetism and magnetically targeted movement. Through enhanced permeability and retention effect *in vivo*, MNP are prone to accumulation in tumor tissues [5, 6], allowing application in magnetic hyperthermia [7]. We have previously prepared Alg- $\text{Fe}_3\text{O}_4$ -CDDP [8] which well inhibited tumor cells *in vitro* [9].

However, it was easily barriered in liver and kidney tissues and resistant to CDDP, for which combination therapy is usually required.

MMPs are closely associated with extracellular matrix (ECM), so they play crucial roles in tumor invasion and metastasis. TIMPs maintain the equilibrium of ECM by regulating the activities of MMPs [10]. As the most active endogenous inhibitory factor for MMP-2, TIMP-2 dominates in tumor onset and progression, mainly by suppressing MMP expressions to reduce the invasion capacity, by producing angiogenesis inhibitors to suppress the proliferation of endothelial cells, and by weakening the angiogenesis ability of tumor microenvironment [10, 11]. For example, TIMP-2 expression, which significantly decreases in colon cancer tissues [12], is closely related with degree of differentiation and lymphatic metastasis in gastric cancer cells, i.e. low expression level marks high degree of malignancy [13, 14]. High expression levels of TIMP-2 in breast cancer, bladder cancer and tongue cancer patients indicate good prognosis [15, 16]. All these findings suggest TIMP-2 is applicable to cancer gene therapy in which carriers play essential roles for transfection [17]. Dendritic PEI, as an organic cationic polymer rich in amino groups, has high efficiency for gene transfection. Nevertheless, its application is limited owing to high cytotoxicity [18]. PEG enjoys non-toxicity, high water solubility and compatibility with many organics. PEI, when bound to PEG, can increase the water solubility of the complex, weaken the interaction with proteins in blood, decrease non-specific autophagy of the reticuloendothelial system in the liver and spleen, extend the circulation time *in vivo* and reduce cytotoxicity [19].

Currently, co-delivery of chemotherapeutic agents and genes can synergistically enhance the therapeutic effects, as well as reduce toxicity, side effect and drug resistance of tissues, thus having attracted particular attention worldwide [20]. Physically and chemically stable, evenly dispersed MNP-CDDP/TIMP-2 were prepared through adsorption of TIMP-2 plasmid by MPEG-PEI and encapsulation of MNP-CDDP by electrostatic interaction. The products had the average hydrodynamic particle size of 151.3 nm that met the application requirement of nanodrugs. EE of CDDP was 33.2%. Agarose gel electrophoresis exhibited that the nanocarriers managed to well protect the plasmid.

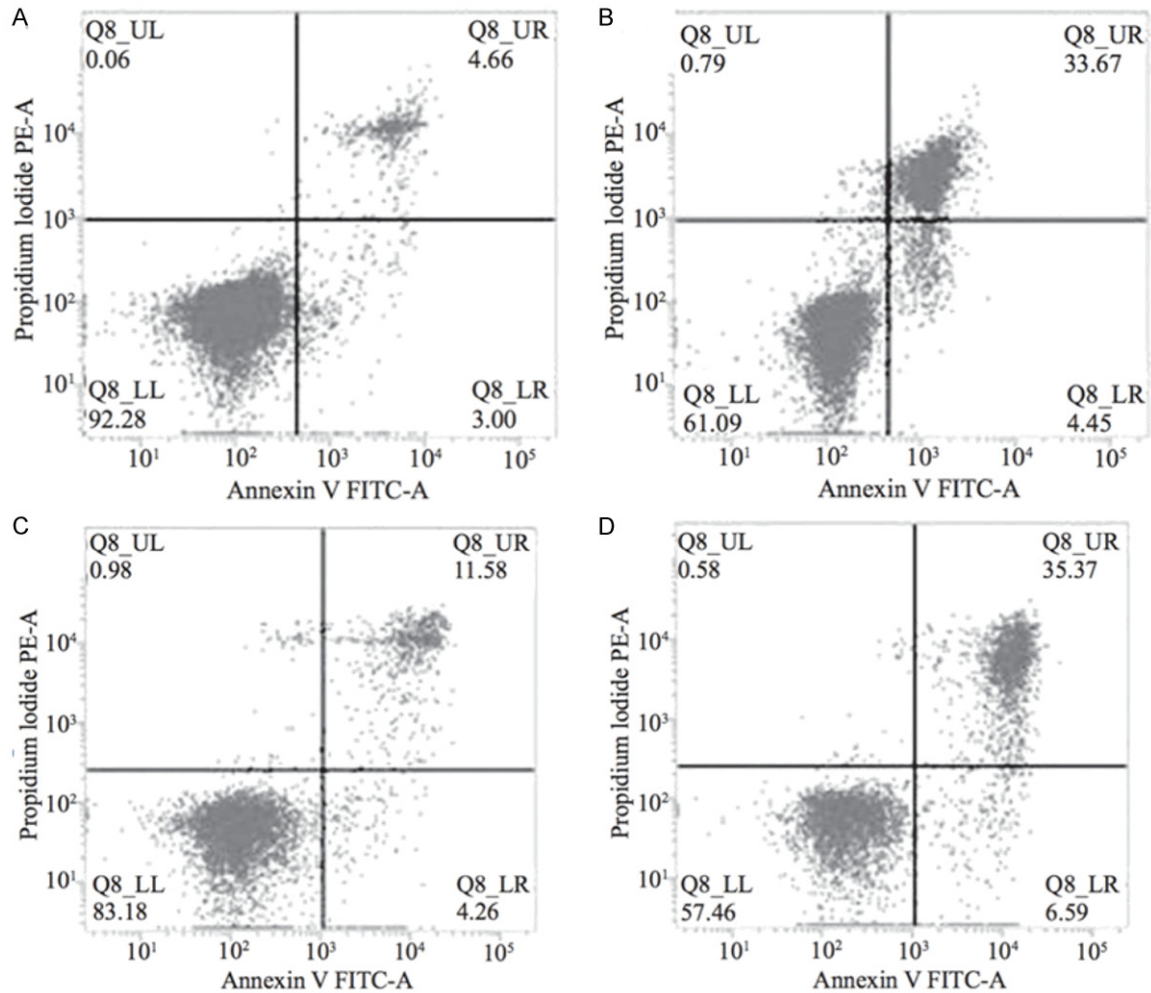


**Figure 8.** Cell apoptosis detected by flow cytometry. A: MNP/(MPEG-PEI) group; B: MNP-CDDP group; C: (MPEG-PEI) TIMP-2 group; D: MNP-CDDP/TIMP-2 group.

Appropriate PEGylation is able to augment the transfection efficiency. MPEG-PEI had the molar ratio of 1:1. RT-PCR and Western blot showed that TIMP-2 mRNA and protein expressions significantly increased in HepG2 cells, indicating that MNP-CDDP successfully mediated the transfection of TIMP-2 plasmid. As evidenced by flow cytometry, the transfection rate of MNP-CDDP/TIMP-2 was 22.9%, which was slightly lower than that of individual PEI. As suggested by CCK-8 assay, flow cytometry and Matrigel invasion assay, the growth inhibition rate, apoptotic rate and invasion capacity of the MNP-CDDP/TIMP-2 group were significantly lower than those of CDDP chemotherapy or TIMP-2 gene therapy alone. Hence, CDDP and TIMP-2 in MNP-CDDP/TIMP-2 synergistically exerted inhibitory effects on HepG2 cells.

In summary, magnetic nanoparticles co-carrying TIMP-2 and CDDP were successfully prepared, which managed to inhibit the proliferation of HepG2 cells and to facilitate their apoptosis. Combining TIMP-2 with CDDP enhanced the antitumor effects, probably allowing simultaneous chemotherapy and gene therapy *in vitro*. Future studies are ongoing in our group to fabricate specific chemotherapeutic agents carrying nanogenes targeting liver cancer cells, as well as to make progress on intracellular molecular targeted therapy.

#### Acknowledgements

This study was financially supported by the National Natural Science Foundation of Xinjiang Autonomous Region.

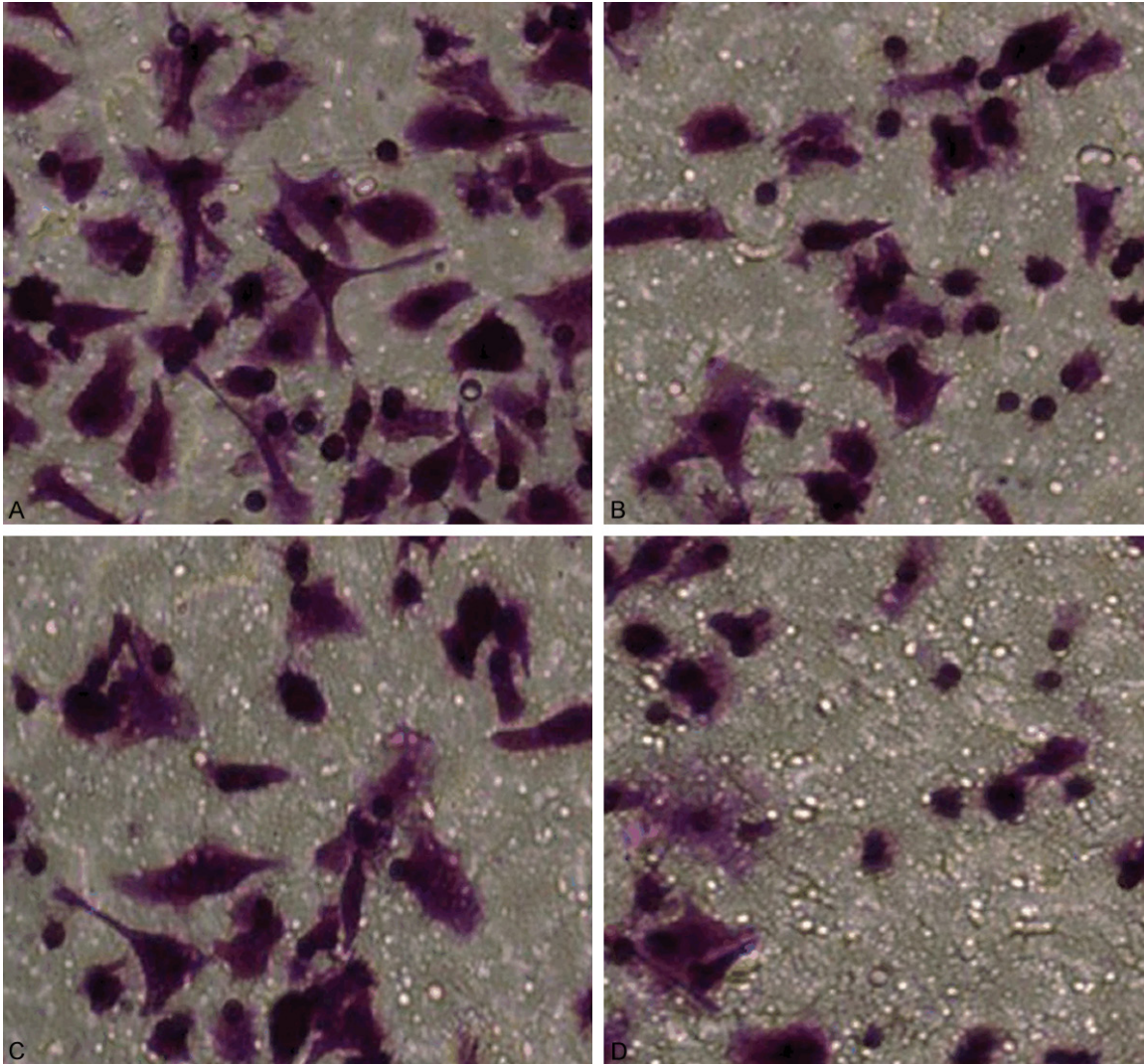


**Figure 9.** Matrigel invasion assay of HepG2 cells (100 × magnification). A: MNP/(MPEG-PEI) group; B: MNP-CDDP group; C: (MPEG-PEI) TIMP-2 group; D: MNP-CDDP/TIMP-2 group.

#### Disclosure of conflict of interest

None.

**Address correspondence to:** Yuexin Zhang, Department of Infectious Diseases, First Affiliated Hospital of Xinjiang Medical University, Urumqi 830054, P. R. China. E-mail: zhangyuexindid@yeah.net

#### References

- [1] Parkin DM, Bray F, Ferlay J, Pisani P. Estimating the world cancer burden: Globocan 2000. *Int J Cancer* 2001; 94: 153-6.
- [2] Bourboulia D, Han H, Jensen-Taubman S, Gavil N, Isaac B, Wei B, Neckers L, Stetler-Stevenson WG. TIMP-2 modulates cancer cell transcrip-

tional profile and enhances E-cadherin/beta-catenin complex expression in A549 lung cancer cells. *Oncotarget* 2013; 4: 163-73.

- [3] Li H, Lindenmeyer F, Grenet C, Opolon P, Menashi S, Soria C, Yeh P, Perricaudet M, Lu H. AdTIMP-2 inhibits tumor growth, angiogenesis, and metastasis, and prolongs survival in mice. *Hum Gene Ther* 2001; 12: 515-26.
- [4] Li ZH, Xie MQ, Chen SJ, Wang L. Complexing cis-diaminedichloroplatinum-loaded magnetic nano-medicine for treating nasopharyngeal carcinoma *in vitro*. *Journal of Clinical Rehabilitative Tissue Engineering Research* 2009; 29.
- [5] Greish K. Enhanced permeability and retention of macromolecular drugs in solid tumors: a royal gate for targeted anticancer nanomedicines. *J Drug Target* 2007; 15: 457-64.

## Magnetic particles and liver cancer

- [6] Zdrojewicz Z, Waracki M, Bugaj B, Pypno D, Cabala K. Medical applications of nanotechnology. *Postepy Hig Med Dosw (Online)* 2015; 69: 1196-204.
- [7] Baldi G, Ravagli C, Mazzantini F, Loudos G, Adan J, Masa M, Psimadas D, Fragogeorgi EA, Locatelli E, Innocenti C, Sangregorio C, Comes Franchini M. In vivo anticancer evaluation of the hyperthermic efficacy of anti-human epidermal growth factor receptor-targeted PEG-based nanocarrier containing magnetic nanoparticles. *Int J Nanomedicine* 2014; 9: 3037-56.
- [8] Xie MQ, Chen SJ, Xu XQ, Li ZH, Shen H, Xu JR. [Preparation of two types of cisplatin magnetic nanoparticles and comparison of their characteristics]. *Chinese Science Bulletin* 2005; 19 : 2079-84.
- [9] Hasson H, Warshawsky A. High-performance liquid chromatographic determination of cis-diamminedichloroplatinum (II) (cisplatin) as the o-phenylenediamine complex. *J Chromatogr* 1990; 530: 219-21.
- [10] Jiang Y, Goldberg ID, Shi YE. Complex roles of tissue inhibitors of metalloproteinases in cancer. *Oncogene* 2002; 21: 2245-52.
- [11] Peterson NB, Beeghly-Fadiel A, Gao YT, Long J, Cai Q, Shu XO, Zheng W. Polymorphisms in tissue inhibitors of metalloproteinases-2 and -3 and breast cancer susceptibility and survival. *Int J Cancer* 2009; 125: 844-50.
- [12] Offenberg H, Brunner N, Mansilla F, Orntoft Torben F, Birkenkamp-Demtroder K. TIMP-1 expression in human colorectal cancer is associated with TGF-B1, LOXL2, INHBA1, TNF-AIP6 and TIMP-2 transcript profiles. *Mol Oncol* 2008; 2: 233-40.
- [13] Alakus H, Grass G, Hennecken JK, Bollschweiler E, Schulte C, Drebbler U, Baldus SE, Metzger R, Hölscher AH, Mönig SP. Clinicopathological significance of MMP-2 and its specific inhibitor TIMP-2 in gastric cancer. *Histol Histopathol* 2008; 23: 917-23.
- [14] Zhang JF, He SM, Cai JJ, Cao XJ, Sun RX, Fu Y, Zeng R, Gao W. Preprocessing of tandem mass spectrometric data based on decision tree classification. *Genomics Proteomics Bioinformatics* 2005; 3: 231-7.
- [15] Nakopoulou L, Giannopoulou I, Lazaris A, Alexandrou P, Tsirmpa I, Markaki S, Panayotopoulou E, Keramopoulos A. The favorable prognostic impact of tissue inhibitor of matrix metalloproteinases-1 protein overexpression in breast cancer cells. *APMIS* 2003; 111: 1027-36.
- [16] Olson MW, Gervasi DC, Mobashery S, Fridman R. Kinetic analysis of the binding of human matrix metalloproteinase-2 and -9 to tissue inhibitor of metalloproteinase (TIMP)-1 and TIMP-2. *J Biol Chem* 1997; 272: 29975-83.
- [17] Ibraheem D, Elaissari A, Fessi H. Gene therapy and DNA delivery systems. *Int J Pharm* 2014; 459: 70-83.
- [18] Godbey WT, Wu KK, Mikos AG. Poly (ethylenimine) and its role in gene delivery. *J Control Release* 1999; 60: 149-60.
- [19] Kichler A, Chillon M, Leborgne C, Danos O, Frisch B. Intranasal gene delivery with a poly-ethylenimine-PEG conjugate. *J Control Release* 2002; 81: 379-88.
- [20] Ma D, Zhang HB, Chen YY, Lin JT, Zhang LM. New cyclodextrin derivative containing poly (L-lysine) dendrons for gene and drug co-delivery. *J Colloid Interface Sci* 2013; 405: 305-11.